UCLA
COMPUTATIONAL AND APPLIED MATHEMATICS

Second Order Differential Functionals in Total Variational-Based Image Restoration

Tony Chan
Antonio Marquina
Pep Mulet

August 1998

CAM Report 98-35

Department of Mathematics
University of California, Los Angeles
Los Angeles, CA. 90095-1555

SECOND ORDER DIFFERENTIAL FUNCTIONALS IN TOTAL VARIATION-BASED IMAGE RESTORATION

TONY CHAN*, ANTONIO MARQUINA† AND PEP MULET†

Abstract. The Total Variation (TV) denoising methods is a PDE-based technique that preserves edges well but has the sometimes undesirable *staircase effect*, namely the transformation of smooth regions (*ramps*) into piecewise constant regions (*stairs*). In this paper we present an improved model constructed by adding a nonlinear second order differential term to the TV functional that substantially reduces the staircase effect, while preserving sharp jump discontinuities (edges). We have experimentally found that this new second order term alone can produce solutions with sharp edges. We show numerical evidence of the power of resolution of this novel model with respect to the TV model in some 1D and 2D numerical examples.

1. Introduction. The degradation of an image is usually unavoidable during its acquisition and at the early stages of its processing and it renders difficult and inaccurate the latter phases. The classical algorithms for image denoising have been mainly based on least squares and, consequently, their outputs may be contaminated by Gibbs phenomena and do not approximate well images containing edges. To overcome this difficulty a technique based on the minimization of the Total Variation (TV) norm is proposed in [10]. This technique preserves edges well, but the images resulting of the application of this technique in the presence of noise are often piecewise constant, thus the finer details in the original image may not be recovered satisfactorily and that *ramps* (affine regions) will give *stairs* (piecewise constant regions), see Fig. 8.2. In this paper we propose the addition of a nonlinear second order differential term to the TV functional that substantially reduces the staircase effect, while preserving sharp jump discontinuities (edges). Actually, we have experimentally found that this new second order term by itself can produce solutions of the denoising problem with sharp edges.

The paper is organized as follows: in section 2, we describe the original TV model and the nonlinear equations associated to it. In section 3, we describe the staircase effect caused by the TV model and briefly review several techniques proposed in the literature to deal with it. In section 4, the novel regularizing functional is introduced in a general setting. In section 5, we present an analysis of the new model in the one-dimensional case and discuss some stability issues and possible methods for its solution. In section 6, a straightforward two-dimensional extension of the one-dimensional functional is explored, and more sophisticated possibilities are hinted. We comment on the choice of parameters in 7. Finally, in section 8, we discuss some numerical techniques to solve the problem and present numerical experiments comparing the results of the total variation and the new models.

2. Total variation denoising. An image can be interpreted as either a real function defined on Ω, a bounded and open domain of $\mathbb{R}^2$, (for simplicity we will

*Department of Mathematics, University of California, Los Angeles, 405 Hilgard Avenue, Los Angeles, CA 90024-1555. E-mail address: chan@math.ucla.edu. URL: http://www.math.ucla.edu/~chan. Supported by grants ONR-N00014-96-1-0277, NSF DMS-96-26755 and NSF INT9602089.

†Department of Mathematics, University of California, Los Angeles, 405 Hilgard Avenue, Los Angeles, CA 90024-1555 and Departament de Matemàtica Aplicada, Universitat de València, Dr. Moliner, 50, 46100 Burjassot, Spain. E-mail addresses: {mulet,marquina}@uv.es, URL's: http://gata.uv.es/~{mulet,marquina}. Supported by NSF grants INT9602089 and DGICYT grant PB94-0987.

assume Ω to be the unit square henceforth) or as a suitable discretization of this continuous image.

Our interest is to restore an image which is contaminated with noise, in such a way that the process should recover the edges of the image. Let us denote by z the observed image and u the real image. The model of degradation we assume is $u + n = z$, where n is a Gaussian white noise, i.e., the values n_i of n at the pixels i are independent random variables, each with a Gaussian distribution of zero mean and variance σ^2 .

Our objective is to estimate u from statistics of the noise and some *a priori* knowledge of the image (smoothness, existence of edges). This knowledge is incorporated into the formulation by using a functional R that measures the quality of the image u, in the sense that smaller values of $R(u)$ correspond to better images. The process, in other words, consists in the choice of the best quality image among those matching the constraints imposed by the statistics of the noise.

The usual approach consists in solving the following constrained optimization problem:

$$\begin{aligned} &\min_u R(u) \\ &\text{subject to } ||u - z||^2_{\mathcal{L}^2} = |\Omega|\sigma^2, \end{aligned} \tag{2.1}$$

since $n = z - u$ and $E(\int_\Omega n^2\, dx) = |\Omega|\sigma^2$ ($E(X)$ denotes the expectation of the random variable X) give that $||u - z||^2_{\mathcal{L}^2} = \int_\Omega (u - z)^2\, dx \approx |\Omega|\sigma^2$.

Examples of regularization functionals that can be found in the literature are, $R(u) = \|u\|_{\mathcal{L}^2}, \|\Delta u\|_{\mathcal{L}^2}, \|\nabla u \cdot \nabla u\|_{\mathcal{L}^2}$, where ∇ is the gradient and Δ is the Laplacian, see Refs. [12, 8]. The main disadvantage of using these functionals is that they do not allow discontinuities in the solution, therefore the edges can not be satisfactorily recovered.

In [10], the *Total Variation norm* or *TV-norm* is proposed as regularization functional for the image restoration problem:

$$TV(u) = \int_\Omega |\nabla u|\, dx = \int_\Omega \sqrt{u_x^2 + u_y^2}\, dx. \tag{2.2}$$

The TV norm does not penalize discontinuities in u, and thus allows us to recover the edges of the original image. The restoration problem can be thus written as

$$\begin{aligned} &\min_u \int_\Omega |\nabla u|\, dx, \\ &\text{subject to } \frac{1}{2}\Big(\int_\Omega (u - z)^2\, dx - |\Omega|\sigma^2\Big) = 0. \end{aligned} \tag{2.3}$$

Its Lagrangian is

$$\int_\Omega |\nabla u|\, dx + \frac{\lambda}{2}\Big(\int_\Omega (u - z)^2\, dx - |\Omega|\sigma^2\Big) \tag{2.4}$$

and its Euler-Lagrange equations, with homogeneous Neumann boundary conditions for u, are:

$$0 = -\nabla \cdot \left(\frac{\nabla u}{|\nabla u|}\right) + \lambda(u - z) \tag{2.5}$$

$$0 = \frac{1}{2}\Big(\int_\Omega (u - z)^2\, dx - |\Omega|\sigma^2\Big). \tag{2.6}$$

There are known techniques (see [3]) for solving the constrained optimization problem (2.3) by exploiting solvers for the corresponding unconstrained problem, whose Euler-Lagrange equations are (2.5) for λ fixed. Therefore, for the sake of clarity, we will assume the Lagrange multiplier λ to be known throughout the exposition. For $\alpha = \frac{1}{\lambda}$, we can then write the equivalent unconstrained problem

$$\min_u \int_\Omega (\alpha|\nabla u| + \frac{1}{2}(u-z)^2)\,dx \tag{2.7}$$

and its Euler-Lagrange equation in the more customary fashion:

$$0 = -\alpha\nabla\cdot\left(\frac{\nabla u}{|\nabla u|}\right) + u - z. \tag{2.8}$$

Since this equation is not well defined at points where $\nabla u = 0$, due to the presence of the term $1/|\nabla u|$, it is common to slightly perturb the Total Variation functional to become:

$$\int_\Omega \sqrt{|\nabla u|^2 + \beta}\,dx, \tag{2.9}$$

where β is a small positive parameter, or,

$$\int_\Omega |\nabla u|_\beta\,dx, \tag{2.10}$$

with the notation ($x \in \mathbb{R}$, $v \in \mathbb{R}^2$)

$$|x|_\beta = \sqrt{x^2+\beta}, \quad |v|_\beta = \sqrt{|v|^2+\beta}. \tag{2.11}$$

In [1] it is shown that the solutions of the perturbed problems

$$\min_u \int_\Omega (\alpha|\nabla u|_\beta + \frac{1}{2}(u-z)^2)\,dx \tag{2.12}$$

converge to the solution of (2.7) when $\beta \to 0$.

3. The staircase effect. The image restoration model based on the Total Variation tends to yield piecewise constant images, i.e., "blocky" images. Whereas this is certainly useful for many applications, it can be a serious drawback for many others. In particular, when applying this denoising technique to an affine image degraded with noise, the result will invariably be a "staircase", thus creating over-sharpening at smooth transitions, see Fig. 8.2 left.

To prevent the TV over-sharpening, one could penalize jumps more. This can be achieved by taking second derivatives into account: intuitively, in discrete form, the first derivative at a height 1 jump of a step function is $\frac{1}{h}$, whereas the second derivative is $\frac{1}{h^2} \gg \frac{1}{h}$ when $h \approx 0$. Somehow, the TV functional does not distinguish between jumps and smooth transitions, therefore we want to analyze functionals that take into account second order derivatives. Successful application of functionals with second (or higher) order derivatives can be found in work of Geman and Reynolds (see [7]) and Chambolle and Lions ([5]). In [4], Blomgren, Chan and Mulet propose a "TV-H^1 interpolation" approach that avoids the use of second order derivatives to address the staircase problem of the TV technique.

We briefly review the inf-convolution technique of Chambolle and Lions and refer the reader to [5] for further information. Chambolle and Lions propose to use as regularizing functional the *inf-convolution* of the TV functional F_1, and a functional based on second order derivatives

$$F_2 = \alpha \int_\Omega |d^2 u| \, dx, \tag{3.1}$$

where d^2u is the second differential of u and α is a parameter that balances F_1 and F_2. The problem can then be written as finding $u = u_1 + u_2$ such that

$$\begin{aligned} (u_1, u_2) = \underset{u_1, u_2}{\operatorname{argmin}} \, & F_1(u_1) + F_2(u_2) \\ \text{subject to } & \frac{1}{2}(\|u_1 + u_2 - z\|_{\mathcal{L}^2} - \sigma^2) = 0. \end{aligned} \tag{3.2}$$

In other words, this method decomposes u into a sum of a smooth function u_2 and a function u_1 that contains the jumps, so that the corresponding Euler-Lagrange equations are solved by u_1, u_2.

4. Our proposed second order model. Our goal is to get a functional of the form

$$R(u) = \int_\Omega f(u, \nabla u, \mathcal{L}(u)) \, dx, \tag{4.1}$$

for a real function $f(p, q, r)$ and an elliptic operator $\mathcal{L}(u)$, that retains the good properties of the TV functional near the "true" edges, while penalizing "wrong" edges created in regions which should be smooth. The naive choice of, e.g.,

$$f(u, \nabla u, \mathcal{L}(u)) = \alpha |\nabla u| + \mu (\mathcal{L}(u))^2 + \frac{1}{2}(u - z)^2, \tag{4.2}$$

results in a high global penalization of jumps that smoothes the data excessively. An adaptive scheme would then be needed. We propose a functional defined by

$$f(u, \nabla u, \mathcal{L}(u)) = \alpha |\nabla u|_\beta + \mu \Phi(|\nabla u|)(\mathcal{L}(u))^2 + \frac{1}{2}(u - z)^2, \tag{4.3}$$

where Φ is a real function that indicates the presence of edges, in the sense that its value approaches 0 when $|\nabla u|$ is large, i.e. near edges.

The motivation for the choice of this precise form for the additional second order term is that it is quadratic in $\mathcal{L}(u)$, hence the numerical treatment is easier than merely choosing $|\mathcal{L}(u)|$. The additional complexity caused by the term $\Phi(|\nabla u|)$ in (4.3) does not render it much more complicated than (4.2), for this equation is already non-quadratic.

A family of functions that meet the above requirements is $\Phi(x) = 1/(\sqrt{x^2 + 1})^p$ $(p > 0)$, which can be written more compactly as $1/|x|_1^p$, using the notation introduced in (2.11). A balance between the two differential terms of (4.3) can be achieved by the choice of exponent $p = 3$, for then both depend on the scale h as $\mathcal{O}(\frac{1}{h})$, thus making the functional $R(u)$ independent of the scale h: intuitively,

$$\alpha |\nabla u|_\beta + \mu \frac{\mathcal{L}(u)^2}{|\nabla u|_1^p} \approx \mathcal{O}(h^{-1}) + \frac{\mathcal{O}((\frac{1}{h^2})^2)}{\mathcal{O}(\frac{1}{h^p})} \approx \mathcal{O}(h^{-1}) + \mathcal{O}(h^{p-4}), \tag{4.4}$$

which gives $p = 3$, by equating the exponents of both terms. We will henceforth write the functional in (4.3) with the function $\Phi(x) = \frac{1}{|x|_1^3}$.

A drawback of using the functional in (4.3) to solve variational problems is that it is not convex, therefore some good mathematical properties of convex functionals, as uniqueness of solutions, are not present. However, we have numerical evidence that our algorithms applied to solve a suitable regularization of the Euler-Lagrange equations converge to a well defined solution. Non convex functionals are quite common in the image processing field (see [7, 13, 2]).

5. The one-dimensional model. With the reasonable choice of $\mathcal{L}(u) = u''$, the Euler-Lagrange equation for the variational problem

$$\int_0^1 f(u, u', u'')\, dx, \tag{5.1}$$

are

$$0 = (f_{u''})'' - (f_{u'})' + f_u. \tag{5.2}$$

For the case of

$$f(u, u', u'') = \alpha |u'|_\beta + \mu \frac{(u'')^2}{|u'|_1^3} + \frac{1}{2}(u - z)^2, \tag{5.3}$$

this equation reads:

$$\begin{aligned} 0 &= (\kappa_2(u)u'')'' - (\kappa_1^*(u)u')' + u - z \\ \kappa_1^*(u) &= \frac{\alpha}{|u'|_\beta} - 3\mu \frac{(u'')^2}{|u'|_1^5} \\ \kappa_2(u) &= \frac{2\mu}{|u'|_1^3}. \end{aligned} \tag{5.4}$$

The coefficient κ_2 is strictly positive, whereas k_1 may be negative. This can be problematic when solving discretizations of these equations, for then it may cause numerical difficulties due to the lack of maximum principles for this fourth order equation. Near the jump discontinuities of u, $k_2(u)$ becomes $O(h^3)$ and $k_1(u)$ is about $O(h)$ (h being the spatial step-size of the representation of u), thus the second order term dominates the equation, and therefore the positivity of the coefficient $k_1(u)$ is an unavoidable requirement to prevent the increasing in total-variation of u that would otherwise make the solution of (5.4) ill-conditioned. Therefore, we introduce a regularization, consisting in redefining κ_1^* to be $\kappa_1 = \frac{\alpha}{|u'|_\beta} > 0$, which can be interpreted as adding a *non-linear viscosity* to the original equation. To recap, the regularized equations that we propose are:

$$\begin{aligned} 0 &= (\kappa_2(u)u'')'' - (\kappa_1(u)u')' + u - z \\ \kappa_1(u) &= \frac{\alpha}{|u'|_\beta} \\ \kappa_2(u) &= \frac{2\mu}{|u'|_1^3}. \end{aligned} \tag{5.5}$$

Note that if $\alpha = 0$ we still have a fourth order anisotropic diffusion equation with denoising effect.

This regularization makes the equation satisfy a local maximum principle in the sense that suitable discretizations give positive definite frozen Jacobians. Near the jumps the model approaches the TV model, since the coefficient $\kappa_2 = \frac{2\mu}{|u'|_1^3}$ of the additional fourth order term behaves as $\mathcal{O}(h^3)$. Furthermore, equation (5.5) can be regarded as adding the fourth order non-linear term $(\kappa_2(u)u'')''$ to the Euler-Lagrange equations (2.8). It is worthwhile to point out that, due to the lack of symmetry, (5.5) is not the Euler-Lagrange equation of any variational problem.

For the numerical solution of (5.5), we could consider the steady-state solution of the time evolving equation

$$u_t = -(k_2(u)u_{xx})_{xx} + (k_1(u)u_x)_x - u + z, \tag{5.6}$$

where u is now a function of t and x. The time evolution equation is parabolic since $k_2(u)$ is strictly positive, and we know that the constant coefficient parabolic equation

$$u_t = -a\,u_{xxxx} + b\,u_{xx} - u + z, \tag{5.7}$$

with $a > 0$ and initial data in $\mathcal{L}^2$ is a well-posed problem, (see [9, p. 271]). Equation (5.6) is, of course, much more complicated than (5.7), but this can serve as a model to understand the local behavior of the linear equation obtained after freezing the coefficients of (5.6).

In our case, we have non-linear coefficients that change with u' and u'', so that, time marching procedures are usually stiff and inefficient, as practice have shown in those kind of problems: the CFL stability restriction for explicit schemes (see [9]) requires the time step to be $\mathcal{O}(h^4)$, thus precluding its use in any realistic computation.

The *lagged diffusivity fixed point* iteration has proven lately to be a quite popular linearization method for solving the TV restoration problem, see [14]. In the same fashion, we can consider an iterative procedure that aims to converge to a solution of (5.5), starting from the initial approximation $u_0 = z$ and solving for u^{n+1} the following linear fourth-order elliptic equation at every step:

$$0 = (\kappa_2(u_n)u''_{n+1})'' - (\kappa_1(u_n)u'_{n+1})' + u_n - z, \quad n = 0, 1 \ldots. \tag{5.8}$$

Remark 1. We have observed in our experiments that the second order model for the parameter $\alpha = 0$ and sound choices of μ, i.e.,

$$\begin{aligned} 0 &= (\kappa_2(u)u'')'' + u - z, \\ \kappa_2(u) &= \frac{2\mu}{|u'|_1^3}, \end{aligned} \tag{5.9}$$

can be used for denoising purposes. It recovers sharp edges, does not produce staircasing, but it may create artificial non-null gradients at flat regions and some over/under shooting, that do not appear for sufficiently big α.

6. The two-dimensional model. In the two-dimensional case there are many possible choices for the elliptic operator $\mathcal{L}(u)$, the apparently most suitable one amongst them being that of the *directional Laplacian*

$$\mathcal{L}(u) = \Big(\frac{\nabla u}{|\nabla u|}\Big)^T H(u) \Big(\frac{\nabla u}{|\nabla u|}\Big) = \frac{u_{xx}u_x^2 + 2u_{xy}u_xu_y + u_{yy}u_y^2}{u_x^2 + u_y^2}, \tag{6.1}$$

where $H(u)$ denotes the Hessian matrix of u. However, the Euler-Lagrange equations for the isotropic Laplacian $\mathcal{L}(u) = \Delta u = u_{xx} + u_{yy}$ are easier to tackle numerically,

therefore we will restrict ourselves to treat this case in the sequel, leaving the interesting case of the directional Laplacian for future research.

With the latter choice of elliptic operator and function $\Phi(x) = \frac{1}{|x|_1^3}$, the variational problem reads as follows:

$$\min_u \int_\Omega (\alpha |\nabla u|_\beta + \mu \frac{(\Delta u)^2}{|\nabla u|_1^3} + \frac{1}{2}(u - z)^2), \tag{6.2}$$

and the Euler-Lagrange equations are the following:

$$\begin{aligned} 0 &= \Delta(\kappa_2 \Delta u) - \nabla \cdot (\kappa_1^* \nabla u) + u - z, \\ \kappa_1^* &= \frac{\alpha}{|\nabla u|_\beta} - 3\mu \frac{(\Delta u)^2}{|\nabla u|_1^5}, \\ \kappa_2 &= \frac{2\mu}{|\nabla u|_1^3}. \end{aligned} \tag{6.3}$$

The same stability issues as in the one dimensional case apply here. We drop the negative term in κ_1, thus resulting in an addition of artificial viscosity to (6.3), thus resulting in the equations:

$$\begin{aligned} 0 &= \Delta(\kappa_2 \Delta u) - \nabla \cdot (\kappa_1 \nabla u) + u - z, \\ \kappa_1 &= \frac{\alpha}{|\nabla u|_\beta}, \\ \kappa_2 &= \frac{2\mu}{|\nabla u|_1^3}. \end{aligned} \tag{6.4}$$

As in the one dimensional case, we could use the fixed point scheme

$$0 = \Delta(\kappa_2(u_n)\Delta u_{n+1}) - \nabla \cdot (\kappa_1(u_n)\nabla u_{n+1}) + u_{n+1} - z, \tag{6.5}$$

solving at each iteration a linear fourth order elliptic equation. Nevertheless, in our experiments we have found that it does not show a stable convergence behavior, but a suitable modification of it does converge. The modified scheme consists in solving equation (6.5) for $\hat{u}_{n+1}$ and then under-relax by setting u_{n+1} to be the average $\frac{1}{2}(u_n + \hat{u}_{n+1})$, i.e.

$$\begin{aligned} &\Delta(\kappa_2(u_n)\Delta \hat{u}_{n+1}) - \nabla \cdot (\kappa_1(u_n)\nabla \hat{u}_{n+1}) + \hat{u}_{n+1} = z, \\ &u_{n+1} = \frac{u_n + \hat{u}_{n+1}}{2}. \end{aligned} \tag{6.6}$$

The same issues as in 1D about using equation (6.4) with $\alpha = 0$ apply here as well.

7. Choice of parameters. We comment briefly on the choice of the various parameters in the algorithm described above. The parameter with respect to which the problem is less sensitive, and therefore easier to choose, is β. If d is the dynamic range of the image (i.e. u takes values from the interval $[0, d]$) and h is the spatial discretization length, then we recommend from our experience to use $\beta = 10^{-5}\frac{d^2}{h^2}$, so β scales properly with the term $|\nabla u|^2$ that appears in (2.11).

The other two parameters, α, μ, are more complicated to choose. We describe now a heuristic procedure that has proven to be quite successful in our experiments.

We make the usual assumption that the noise variance σ^2 is known, as is, for example, the setting of [10].

We have observed that the fixed point scheme ((5.8) in 1D and the modified (6.5) in 2D) with $\kappa_1 = 0$ converges nicely for μ less than some threshold value μ_0, but gives numerical trouble (oscillations of the norm of the equations and bad conditioning of the frozen Jacobians) for μ sufficiently bigger than μ_0 ($\mu > 1.5\mu_0$, say). We recommend selecting $\mu = \mu_0$ and then adjusting α so that u matches the noise variance, i.e., $\|u - z\|^2_{\mathcal{L}^2} = \sigma^2$, by using the techniques of [3] or by taking into account that $\|u_\alpha - z\|_{\mathcal{L}^2}$ typically is an increasing function of α, where u_α is the solution of problem for that α.

8. Numerical results. In this section, we perform some numerical comparisons in 1D and 2D between the new model and the total variation model. Throughout this section, the parameter β is set to 10^{-4} and the other parameters are chosen as described in section 7, so that a match of the noise level is achieved. The linear PDE's in (5.8) and (6.6) are discretized by standard forward differences. We have observed that smoothing u, by convolving it with some kernel G, before the computation of $\kappa_2(u) = \frac{2\mu}{|\nabla u|^3}$, namely, setting $\kappa_2(u) = \frac{2\mu}{|\nabla(G*u)|^3}$, substantially improves the convergence behavior of the fixed point scheme. The resulting systems of linear equations (with symmetric and positive definite matrices) are solved by Gaussian elimination in 1D and the conjugate gradient method preconditioned by incomplete Choleski in 2D.

In the first experiment we compare the result of the restoration using the new model with the result of the constrained TV restoration for a number of test 1D images, including piecewise constant, piecewise linear and piecewise parabolic 1D images. The original 1D images are shown in Fig 8.1, left, and the (artificially) degraded 1D images in Fig 8.1, right. The results of the TV denoising method are shown in Fig 8.2, left. We show in 8.2, right, the result of the second order model. We make a final comparison by overlaying the original, TV restoration and second order restoration for some of the test 1D images and we show it in Fig 8.3. We observe that the results obtained by the new model have sharp gradients at the "true" edges, but smooth transitions at ramps, whereas the TV model shows the typical staircase effect.

In the next experiment, we compare the results of the second order model technique to Chambolle-Lions's inf-convolution approach. In Fig 8.4, left, we plot several solutions of the second order model for some μ's differing by power of 2 factors from the parameter $\mu = 3556h^2$ selected by our algorithm. We point out that the solution corresponding to $\mu = 7111h^2$ (topmost one) does not match the noise level, due to the nature of the selection procedure for μ expounded in section 7. In Fig 8.4, right, we display some solutions of the inf-convolution technique for the values of the parameter $\alpha = h^2, 2h^2, \ldots, 32h^2$, where a match with the noise level has been enforced in our algorithms. The conclusion we can draw from this experiment is that the second order technique is quite less sensitive to the parameter choice than the inf-convolution approach, since for the same range of variation of the parameter that controls the intensity of the second order term (μ in our model and α in Chambolle-Lions') our results look much more uniform, without staircasing for the topmost three and with sharp edges for all of them, whereas the visually best result of the inf-convolution technique, corresponding to $\alpha = 4$, does not contain staircasing, but some spurious gradients have been created in zones that should be flat. Actually, for $\mu = 222h^2$ (at the bottom, $\mu = \frac{1}{16} \times 3556h^2$) only a mild staircase effect appears in the results

of our model. Furthermore, the heuristics applied to the choice of the parameter μ explained in section 7 apparently give good results.

In Fig. 8.5 we compare the results of our second order model with $\alpha = 0$ and $\alpha \neq 0$. This comparison backs the statements in Remark 1.

We end the one-dimensional experiments by showing in Fig 8.6 the magnitude of the nonlinear viscosity added in (5.4) to obtain (5.5). We can conclude from this picture that this artificial viscosity is only relevant in smooth zones, therefore has minimal effect in the sharpness of the recovered edges, and that it is relatively small compared to $\kappa_1(u)$. Therefore the solution u of (5.5) is "close" to be a solution of (5.4), empirically justifying that the latter is an approximation for the former.

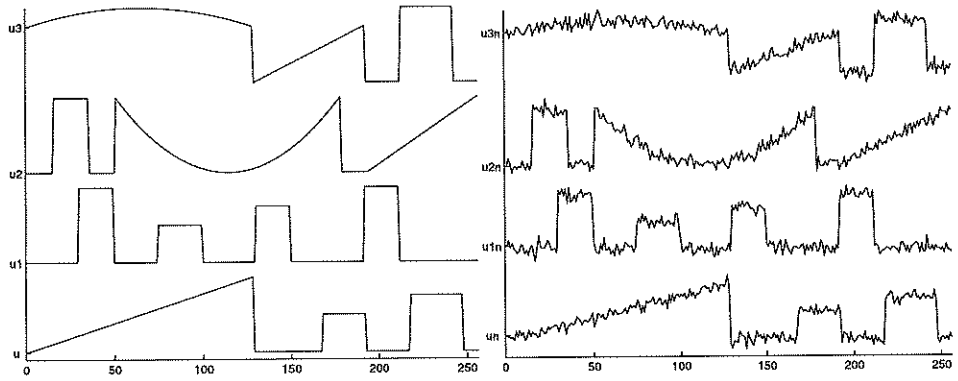

FIG. 8.1. *Left, original 1D images; right noisy 1D images, SNR≈ 5*

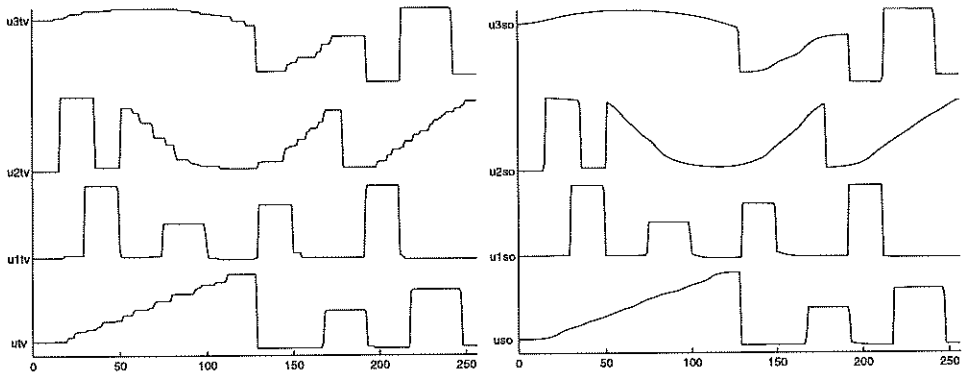

FIG. 8.2. *Left, results of TV restoration; right, results of second order model*

The image of Fig 8.7 is used in the two-dimensional experiment. The SNR of the noisy image is approximately 4. Details of the solutions of the TV and second order restoration problems are shown in Fig. 8.8. The contour plots of these details are shown in Fig 8.9. We can deduce from these contours that the image obtained by the new model is significantly smoother at smooth regions than the one obtained by the TV model, while the "true" edges are preserved similarly by both models. Furthermore, we can see from the contours of the TV restoration that it contains many regions of constant gray level, whereas the new model tends to preserve better some small details, thus giving the restored image a less cartoon-like aspect.

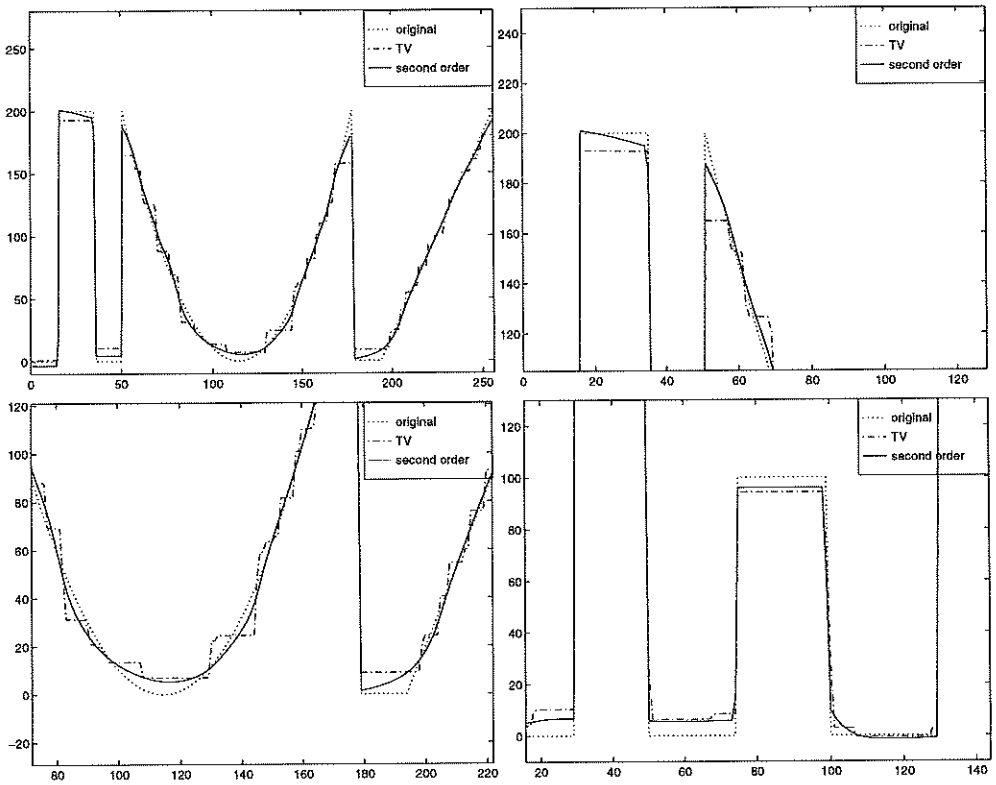

FIG. 8.3. *Details of comparison of TV and second order models*

9. Concluding remarks. The main advantage of the second order model that we have presented in this paper with respect to the original TV model is that it allows smooth transitions without penalizing sharp edges. It also shows significant robustness to the choice of the parameter μ. A disadvantage of the new model is that it has two parameters instead of one, although some heuristics can be applied to choose the additional parameter μ (see section 7). Another disadvantage is that the mathematical problem is much more challenging. In principle, the new functional is not convex, so the uniqueness of the solution of the minimization problem is not ensured. Nevertheless, we have observed that for sound choices of the parameter μ, the fixed point method that we use to solve equation (5.5) or (6.3) converges to the same solution, regardless of the initial approximation. However, this fixed point scheme does not seem to behave as smoothly as in the TV restoration problem. We will pursue more sophisticated and faster alternatives to this method in our future research.

REFERENCES

[1] R. ACAR AND C. R. VOGEL, *Analysis of total variation penalty methods for ill-posed problems*, Inverse Problems, 10 (1994), pp. 1217–1229.

[2] G. AUBERT AND L. VESE, *A variational method in image recovery*, SINUM, 34 (1997), pp. 1948–1979.

[3] P. BLOMGREN AND T. CHAN, *Modular solvers for constrained image restoration problems*, Tech. Rep. CAM report 97-52, Math Department, UCLA, November 1997.

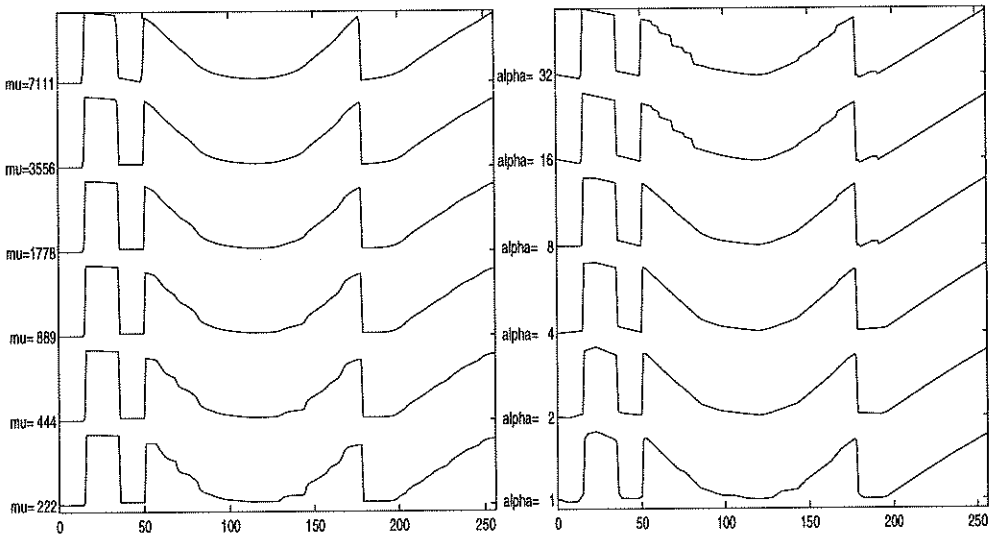

FIG. 8.4. *Comparison of second order and inf-convolution models for several parameters*

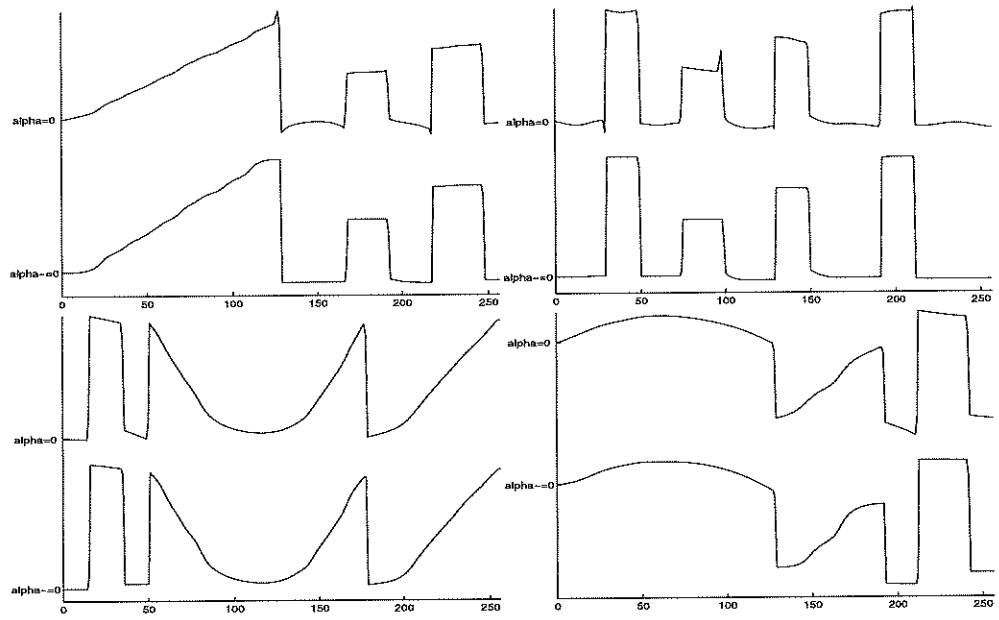

FIG. 8.5. *Comparison of second order model with* $\alpha = 0$ *and* $\alpha \neq 0$.

[4] P. BLOMGREN, T. F. CHAN, AND P. MULET, *Extensions to total variation denoising*, in Proc. SPIE 97, San Diego, 1997.

[5] A. CHAMBOLLE AND P.-L. LIONS, *Image recovery via total variation minimization and related problems*, Tech. Rep. 9509, CEREMADE, 95.

[6] T. CHAN, G. GOLUB, AND P. MULET, *A nonlinear primal-dual method for total variation-based image restoration*, SISC, (1998). To appear.

[7] D. GEMAN AND G. REYNOLDS, *Constrained restoration and the recovery of discontinuities*, IEEE Trans. on Pat. An. and Mach. Intel., 14 (1992), pp. 367–383.

[8] C. W. GROETSCH, *The Theory of Tikhonov Regularization for Fredholm Integral Equations of*

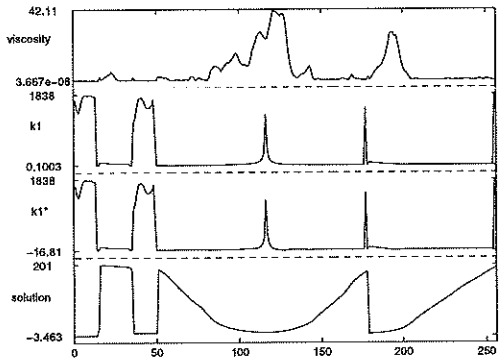

FIG. 8.6. *From bottom to top: solution u of the second order model, diffusion coefficient $\kappa_1^*(u)$ of (5.4), diffusion coefficient $\kappa_1(u)$ of (5.5), nonlinear viscosity added to $\kappa_1^*(u)$ to obtain $\kappa_1(u)$*

FIG. 8.7. *Left: original image, right: noisy image, SNR$\approx$ 4.*

the First Kind, Pitman, Boston, 1984.

[9] B. GUSTAFFSON, H. O. KREISS, AND J. OLIGER, *Time dependent problems and difference methods*, Interscience, J. Wiley, New York, 1995.

[10] L. RUDIN, S. OSHER, AND E. FATEMI, *Nonlinear total variation based noise removal algorithms*, Physica D, 60 (1992), pp. 259–268.

[11] D. STRONG, *Adaptive Total Variation Minimizing Image Restoration*, PhD thesis, Math Department, UCLA, 1997. Published as UCLA CAM report 97-38.

[12] A. N. TIKHONOV AND V. Y. ARSENIN, *Solutions of Ill-Posed Problems*, John Wiley, New York, 1977.

[13] L. VESE, *Variational problems and PDE's for image analysis and curve evolution*, PhD thesis, University of Nice, 1996.

[14] C. R. VOGEL AND M. E. OMAN, *Iterative methods for total variation denoising*, SIAM J. Sci. Statist. Comput., 17 (1996), pp. 227–238.

FIG. 8.8. *Left: image obtained by TV restoration model, right: image obtained by second order model.*

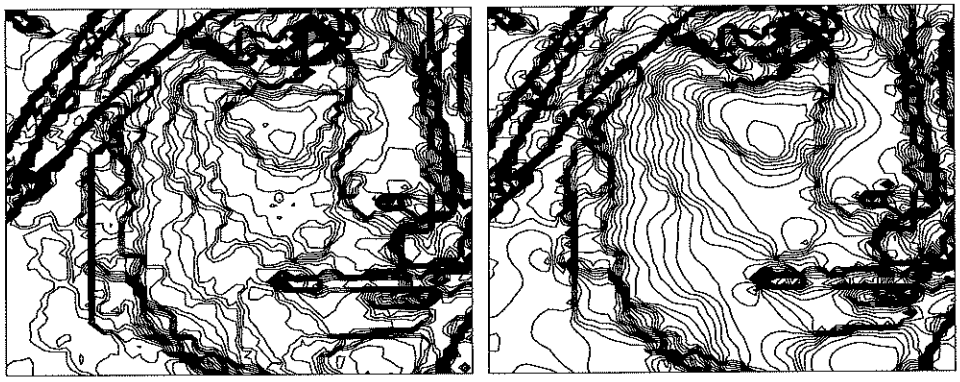

FIG. 8.9. *Left: contours of part of the image obtained by TV restoration model, right: contours of part of the image obtained by new restoration model.*